Acs	600	D	S	L	P	K	T	R	S	G	K	I	M	R	612
PrpE	583	S	Q	L	P	K	T	R	S	G	K	M	L	R	595
Acs2p	628	R	D	L	P	R	T	R	S	G	K	I	M	R	640
luciferase	520	D	E	V	P	K	G	L	T	G	K	L	D	A	532
GrsA	508	D	K	M	P	L	T	S	N	G	K	I	D	R	520
CepA A1	470	D	A	L	P	L	T	A	N	G	K	V	D	R	482
CepA A2	1490	D	A	L	P	L	T	A	H	G	K	I	D	R	1502
CepA A3	3022	D	A	L	P	L	T	T	N	G	K	V	D	R	3034
cda PSI A1	1059	P	R	L	P	V	T	P	N	G	K	L	D	R	1071
cda PSI A2	2169	D	V	L	P	L	T	P	N	G	K	L	D	T	2181
cda PSI A3	3234	D	A	L	P	L	T	L	N	G	K	L	D	R	3246
cda PSI A4	4731	D	A	L	P	L	T	P	N	G	K	L	D	R	4743
cda PSI A5	5771	D	A	L	P	L	T	P	N	G	K	L	D	R	5783
cda PSI A6	6853	D	A	L	P	L	T	P	N	G	K	L	D	R	6865

Fig. 2. Conserved motif containing the acetylation site lysine residue among representative members of the AMP-forming family of proteins. Acs, acetyl-CoA synthetase (gi: 16767525, *S. enterica*); PrpE, propionyl-CoA synthetase (gi: 14917034, *S. enterica*); Acs2p, acetyl-CoA synthetase (gi: 6323182, *Saccharomyces cerevisiae*); GrsA, gramicidin S synthetase I (gi: 3334467, *Brevibacillus brevis*); CepA, one of three subunits that synthesizes chloroeremomycin (European Molecular Biology Laboratory accession numbers X98690 and S46968; gi: 7522085, *Amycolotopsis orientalis*); cda PSI, calcium-dependent antibiotic peptide synthetase I (open reading frame SCO3230, *Streptomyces coelicolor*). We used the motif PX_4GK to identify putative substrates of sirtuins. gi, GenInfo Identifier.

residue of a conserved motif in the family of AMP-forming enzymes (Fig. 2).[5] Lys^{592} of propionyl-CoA synthetase, Lys^{529} of luciferase, and Lys^{517} of gramicidin synthetase 1 (equivalent to Lys^{609} of Acs) are essential for synthesis of the corresponding AMP reaction intermediate but not for the thioester-forming activity of these enzymes (*10–13*). We propose that acetylation modulates the activity of all the AMP-forming family of enzymes. How these enzymes are acetylated remains an open question.

We provide evidence for a broadened role of sirtuins in cell physiology that includes intermediary metabolism. Our results suggest a mechanism for linking the physiological state of the eukaryotic cell with the acetylation state of histones, a key factor in chromatin silencing and chromosome stability. Several studies implicate sirtuins in life-span control in yeast and metazoans (*14*, *15*). Similarly, manipulation of NAD^+ biosynthetic mechanisms has been shown to affect life-span (*16*). A recent study documenting the effect of caloric restriction on yeast mother cell longevity suggested that the increased longevity was causally associated with increased respiration; this life-span extension was sirtuin dependent (*17*). As the Acs enzyme produces acetyl-CoA, a key metabolite of the Krebs cycle, Acs may represent a target for life-span extension.

References and Notes

1. C. B. Brachmann *et al.*, *Genes Dev.* **9**, 2888 (1995).
2. D. Moazed, *Curr. Opin. Cell Biol.* **13**, 232 (2001).
3. S. D. Bell, C. H. Botting, B. N. Wardleworth, S. P. Jackson, M. F. White, *Science* **296**, 148 (2002).
4. A. W. Tsang, J. C. Escalante-Semerena, *J. Bacteriol.* **178**, 7016 (1996).
5. V. J. Starai, H. Takahashi, J. D. Boeke, J. C. Escalante-Semerena, *Genetics*, in press.
6. Materials and methods are available as supporting material on *Science* Online.
7. Single-letter abbreviations for the amino acid residues are as follows: A, Ala; C, Cys; D, Asp; E, Glu; F, Phe; G, Gly; H, His; I, Ile; K, Lys; L, Leu; M, Met; N, Asn; P, Pro; Q, Gln; R, Arg; S, Ser; T, Thr; V, Val; W, Trp; and Y, Tyr.
8. A. R. Horswill, J. C. Escalante-Semerena, *Microbiology* **145**, 1381 (1999).
9. P. Berg, *J. Biol. Chem.* **222**, 991 (1956).
10. A. R. Horswill, J. C. Escalante-Semerena, *Biochemistry* **41**, 2379 (2002).
11. Y. Lee, F. S. Esch, M. A. DeLuca, *Biochemistry* **20**, 1253 (1981).
12. B. R. Branchini, M. H. Murtiashaw, R. A. Magyar, S. M. Anderson, *Biochemistry* **39**, 5433 (2000).
13. E. Conti, T. Stachelhaus, M. A. Marahiel, P. Brick, *EMBO J.* **16**, 4174 (1997).
14. S. J. Lin, P. A. Defossez, L. Guarente, *Science* **289**, 2126 (2000).
15. H. A. Tissenbaum, L. Guarente, *Nature* **410**, 227 (2001).
16. R. M. Anderson *et al.*, *J. Biol. Chem.* **277**, 18881 (2002).
17. S. J. Lin *et al.*, *Nature* **418**, 344 (2002).

18. Supported by National Institutes of Health grants GM62203 (J.C.E.-S.) and GM62385 (J.D.B.). V.J.S. was supported by Jerome Stefaniak and Pfizer Predoctoral Fellowships. Mass spectrometry data were obtained with the assistance of C. Bradford at the AB Mass Spectrometry Facility at Johns Hopkins University School of Medicine, which is funded by National Center for Research Resources shared instrumentation grant 1S10-RR14702, the Johns Hopkins Fund for Medical Discovery, and the Institute for Cell Engineering.

Supporting Online Material
www.sciencemag.org/cgi/content/full/298/5602/2390/DC1
Materials and Methods
Figs. S1 to S5
References

22 August 2002; accepted 22 October 2002

A Distinct Signaling Pathway Used by the IgG-Containing B Cell Antigen Receptor

Chisato Wakabayashi,[1]* Takahiro Adachi,[1]* Jürgen Wienands,[2]† Takeshi Tsubata[1]‡

The immunoglobulin G (IgG)–containing B lymphocyte antigen receptor (IgG-BCR) transmits a signal distinct from that of IgM-BCR or IgD-BCR, although all three use the same signal-transducing component, Igα/Igβ. Here we demonstrate that the inhibitory coreceptor CD22 down-modulates signaling through IgM-BCR and IgD-BCR, but not that through IgG-BCR, because of the IgG cytoplasmic tail, which prevents CD22 phosphorylation. These results suggest that the cytoplasmic tail of IgG specifically enhances IgG-BCR signaling by preventing CD22-mediated signal inhibition. Enhanced signaling through IgG-BCR may be involved in efficient IgG production, which is crucial for immunity to pathogens.

B cells express the membrane-bound form of immunoglobulin (mIg) on the surface as a component of the B cell antigen receptor (BCR) (*1*, *2*), and distinct isotypes of mIg are expressed by B cells, depending on their developmental stage. Naïve B cells in the peripheral lymphoid organs express both mIgM and mIgD, whereas memory B cells in spleen and lymph nodes express mostly mIgG. B cells expressing mIgG show an enhanced response to antigen stimulation compared with those expressing mIgM and/or mIgD (*3*), suggesting that IgG-BCR transmits a signal distinct from IgM-BCR or IgD-BCR. However, all mIg isotypes associate with the common BCR signaling component Igα/Igβ, indicating that all BCRs activate the same signaling pathways (*1*, *2*).

IgM-BCR signaling is negatively regulated by inhibitory coreceptors such as CD22 and CD72 (*4–15*), and these coreceptors are suggested to set a signaling threshold for ligation of IgM-BCR. However, little is known about whether these core-

[1]Department of Immunology, Medical Research Institute, Tokyo Medical and Dental University, 113-8510 Tokyo, Japan. [2]Department of Molecular Immunology, Biology III, Freiburg University and Max-Planck-Institute for Immunobiology, D-79108 Freiburg, Germany.

*These authors contributed equally to this work.
†Present address: Department of Biochemistry and Molecular Immunology, University of Bielefeld, D-33615 Bielefeld, Germany.
‡To whom correspondence should be addressed. E-mail: tsubata.imm@mri.tmd.ac.jp

ceptors regulate IgD-BCR and/or IgG-BCR.

K46μmλ, K46δmλ, and K46γ2amλ are transfectants of the B lymphoma line K46 that express mIgM, mIgD, and mIgG, respectively (*16*, *17*). These mIgs of different isotypes contain identical antigen-binding variable (V) regions, specific for the hapten nitrophenol (NP). We first tested whether inhibitory coreceptors could regulate BCR signaling depending on mIg isotypes. Because K46 cells express CD22 but not CD72, the CD22-negative variants K46μv, K46δv, and K46γv were isolated by repeated cell sorting. Subsequently, expression of CD22 or CD72 was reconstituted by transfecting expression plasmids for these molecules (fig. S1). In the transfectants, expression of CD72 reduced antigen-induced phosphorylation of both extracellular signal–regulated kinase 1 and 2 (ERK1 and ERK2), regardless of mIg isotypes (Fig. 1A and fig. S2, A and B). In contrast, CD22 expression reduced ERK phosphorylation in both K46μv and K46δv, but not that in K46γv, suggesting that CD22 fails to down-modulate ERK activation induced by IgG-BCR ligation. The isotype-specific regulation of ERK activity by CD22 was also confirmed by in vitro kinase assay (Fig. 1B). Additionally, antigen-induced Ca^{2+} mobilization was also regulated by CD22 in the same isotype-dependent manner (Fig. 1C and fig. S2C). Indeed, expression of CD22 reduced BCR-mediated Ca^{2+} mobilization in both K46μv and K46δv, but not that in K46γv, whereas CD72 reduced the Ca^{2+} mobilization in K46γv, as well as K46μv and K46δv. Taken together, CD22 but not CD72 regulates BCR signaling in an mIg isotype–specific manner, and signaling through IgG-BCR, but not that through IgM-BCR or IgD-BCR, is resistant to CD22-mediated signal inhibition in K46 cells.

Both CD22 and CD72 contain immunoreceptor tyrosine-based inhibition motifs (ITIMs) in the cytoplasmic region and negatively regulate IgM-BCR signaling by recruiting Src homology 2 domain–containing tyrosine phosphatase–1 (SHP-1) to their phosphorylated ITIMs upon IgM-BCR ligation (*18*, *19*). Consistent with this, both CD22 and CD72 were phosphorylated (Fig. 2), and these phosphorylated coreceptors coprecipitated with SHP-1 upon ligation of IgM-BCR in K46μv transfectants (Fig. 3). When IgG-BCR was ligated on K46γv transfectants, CD72 was efficiently phosphorylated and coprecipitated with SHP-1. In contrast, CD22 was weakly phosphorylated (Fig. 2), and only a small amount of phosphorylated CD22 was associated with SHP-1 (Fig. 3). This is not due to defects in CD22 in K46γvCD22 cells, because retrovirus-mediated expression of NP-specific IgM-BCR (*20*) restored BCR ligation–induced CD22 phosphorylation and SHP-1 recruitment (fig. S3). Rather, phosphorylation of CD22, essential for SHP-1–mediated signal inhibition, is specifically prevented upon ligation of IgG-BCR on K46 cells. To determine whether this observation is restricted to K46 cells, we reconstituted expression of NP-specific IgM-BCR and IgG-BCR using retroviral vectors (*20*) in other B cell lines such as WEHI-279, BAL17, and A20 (fig. S4A)—all of which express endogenous CD22—and primary mouse spleen B cells (fig.

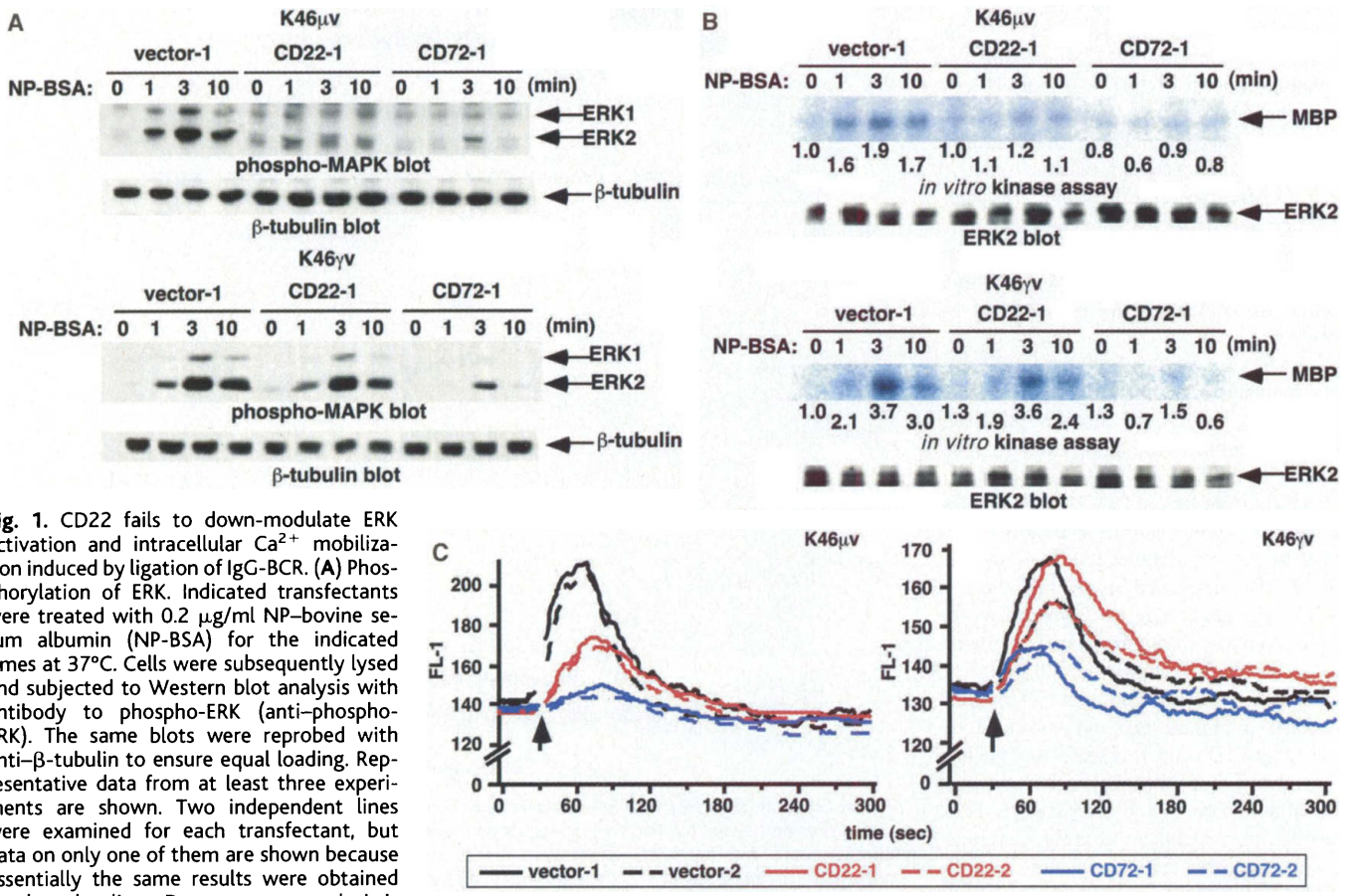

Fig. 1. CD22 fails to down-modulate ERK activation and intracellular Ca^{2+} mobilization induced by ligation of IgG-BCR. (**A**) Phosphorylation of ERK. Indicated transfectants were treated with 0.2 μg/ml NP–bovine serum albumin (NP-BSA) for the indicated times at 37°C. Cells were subsequently lysed and subjected to Western blot analysis with antibody to phospho-ERK (anti–phospho-ERK). The same blots were reprobed with anti–β-tubulin to ensure equal loading. Representative data from at least three experiments are shown. Two independent lines were examined for each transfectant, but data on only one of them are shown because essentially the same results were obtained for the other lines. Dose-response analysis is shown in fig. S2A. (**B**) In vitro kinase assay for ERK2. Indicated transfectants were treated with medium alone or with 0.2 μg/ml NP-BSA for the indicated times at 37°C. Cells were lysed, and ERK2 was immunoprecipitated. Half of the immunoprecipitates were subjected to in vitro kinase assay, using myelin basic protein (MBP) as a substrate. Relative ERK2 activity is indicated. The other half of the ERK2 immunoprecipitates were subjected to Western blot analysis for ERK2 to ensure the presence of ERK2 in the immunoprecipitates. Representative data from three experiments are shown. (**C**) Ca^{2+} mobilization. K46μv and K46γv transfected with the empty vector (black curve), the vector containing CD22 (red curve), or the vector containing CD72 (blue curve) were loaded with Fluo-4/AM, and intracellular free Ca^{2+} was measured by FACSCalibur (Becton Dickinson, Franklin Lakes, NJ). Cells were added with 0.2 μg/ml NP-BSA at 30 s (indicated by arrows), and measurement of free Ca^{2+} was continued for 300 s. Representative data from three experiments are shown.

S4B). In these cells, both CD22 phosphorylation and SHP-1 recruitment were strongly induced by IgM-BCR ligation, but poorly by IgG-BCR ligation (Fig. 4 and fig. S5), in agreement with the results on K46 cells. Moreover, IgG-BCR ligation induced enhanced ERK phosphorylation compared with that induced by IgM-BCR ligation. These results strongly suggest that ligation of IgG-BCR fails to phosphorylate CD22, thereby silencing CD22-mediated signal inhibition by keeping SHP-1 inactive.

IgG, but not IgM or IgD, contains a long cytoplasmic tail, which is conserved in sequence among IgG subtypes and among species (*21*). The cytoplasmic tail of IgG is crucial for efficient IgG production (*22*) and is responsible for the enhanced response of mIgG$^+$ B cells to antigen stimulation (*3*). To assess the role of the cytoplasmic tail of IgG, we infected BAL17 cells with retrovirus to induce expression of chimeras of IgM and IgG (fig. S4A and fig. S5D) because of efficient retrovirus infection of this cell line. Ligation of the IgG/M-BCR containing the extracellular and transmembrane region of IgG and cytoplasmic region of IgM induced strong phosphorylation of CD22 and marked recruitment of SHP-1, as is the case for IgM-BCR ligation (Fig. 4A), suggesting that the cytoplasmic tail of IgG is responsible for preventing CD22-mediated SHP-1 activation. This is confirmed by the finding that ligation of IgM-BCR containing the cytoplasmic region of IgG (IgM/G-BCR) resulted in weak CD22 phosphorylation and poor SHP-1 recruitment, as is the case for IgG-BCR. IgG-BCR thus appears to be protected from CD22-mediated signal inhibition by containing the conserved cytoplasmic tail.

We have demonstrated here that CD22 negatively regulates signaling through IgM-BCR and IgD-BCR, but not that through IgG-BCR. B cells deficient in CD22 alone exhibit hyperreactivity to ligation of IgM-BCR (*11–14*), demonstrating that lack of CD22-mediated negative regulation alone can make B cells hyperreactive to antigen stimulation. Thus, the absence of CD22-mediated signal inhibition of IgG-BCR signaling may be involved in the enhanced response of mIgG$^+$ B cells. Remarkably, the conserved cytoplasmic tail of IgG is responsible for both prevention of CD22-mediated signal inhibition and the enhanced response of IgG$^+$ B cells. It is likely that the IgG tail prevents CD22 phosphorylation essential for signal inhibition, thereby causing IgG-BCR to become more excitable to antigen stimulation. However, the distinct function of IgG-BCR may also involve other, yet unknown properties specific to IgG-BCR. CD22 is expressed on activated B cells such as germinal center B cells and memory B cells (*23*), as well as naïve B cells (*4*). Hyperresponsiveness of IgG-BCR may thus confer upon mIgG$^+$ B cells a growth advantage over mIgM$^+$mIgD$^+$ or mIgM$^+$ B cells in both activated and memory B cell pools. The growth advantage of mIgG$^+$ B cells may be involved in the efficient switching from IgM to IgG production at the cellular level and the efficient response of mIgG$^+$ memory B cells. However, the improved response of memory B cells may also be attrib-

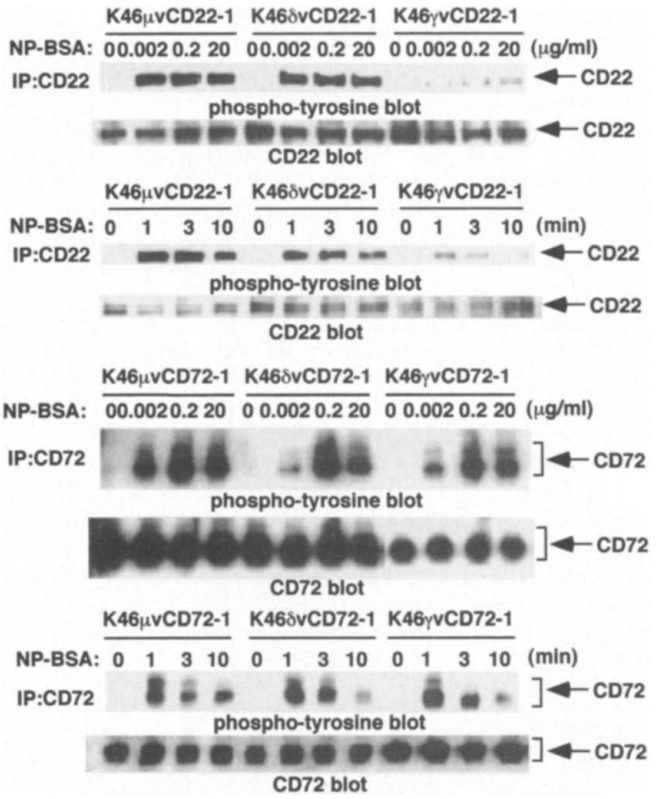

Fig. 2. Ligation of IgG-BCR fails to induce phosphorylation of CD22. CD22 transfectants and CD72 transfectants of K46μv, K46δv, and K46γv were stimulated either with the indicated amounts of NP-BSA for 3 min or with 0.2 μg/ml NP-BSA for the indicated times at 37°C. Cells were lysed, and the lysates were immunoprecipitated with either anti-CD22 or anti-CD72. Immunoprecipitates were subjected to Western blot analysis with anti–phosphotyrosine (4G10). The same blots were reprobed with anti-CD22 or anti-CD72 to ensure equal loading (lower panels). Representative data from at least three experiments are shown.

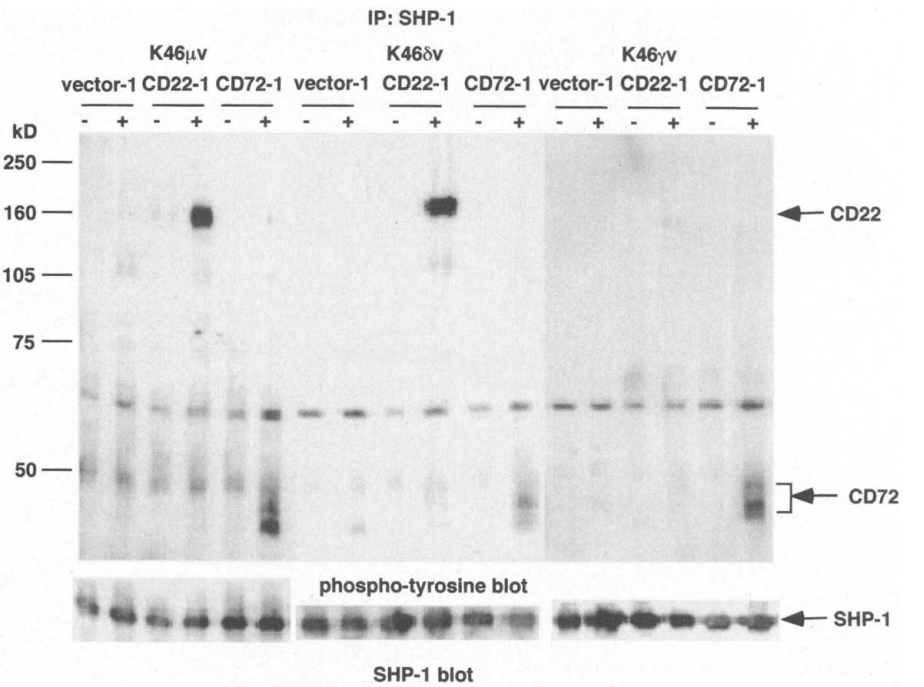

Fig. 3. Ligation of IgG-BCR fails to recruit SHP-1 to CD22. K46μv, K46δv, and K46γv transfected with either empty vector (vector) or vector containing CD22 or CD72 were treated with 0.2 μg/ml NP-BSA for 3 min at 37°C. Cells were lysed, and the lysates were immunoprecipitated with anti–SHP-1. The immunoprecipitates were analyzed by Western blotting with anti–phosphotyrosine (4G10). The positions for CD22 and CD72 are indicated. The positions are determined by the size and presence of the bands specifically in the CD22 or CD72 transfectants. The blot was reprobed with anti–SHP-1 to ensure the presence of SHP-1 in the immunoprecipitates (lower panels). Representative data from at least three experiments are shown.

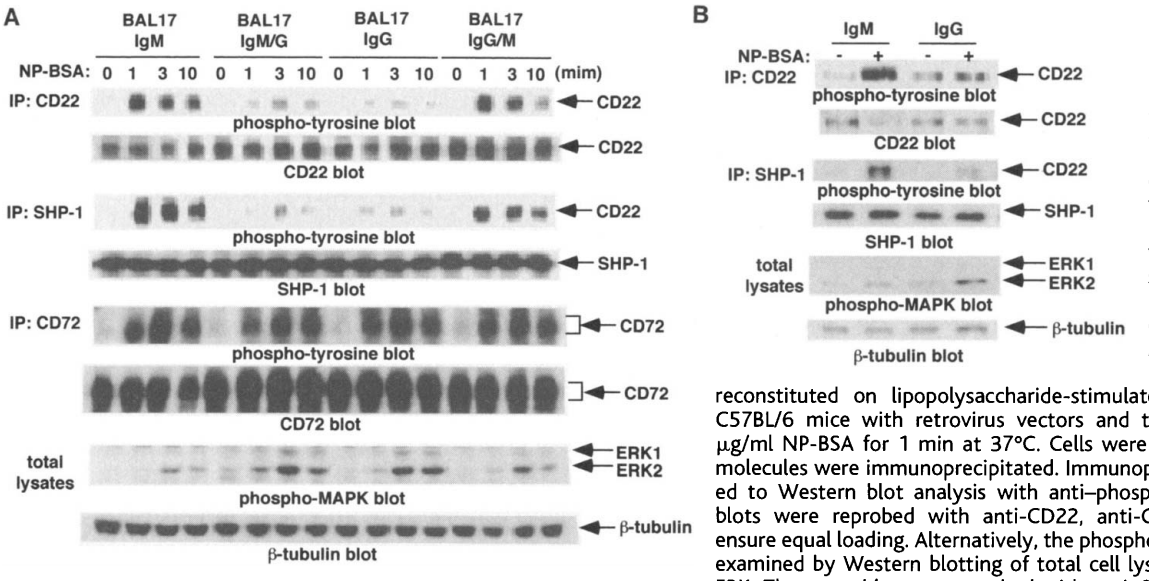

Fig. 4. CD22 regulates BCR signaling in an isotype-specific manner in the B cell line BAL17 and mouse spleen B cells. (**A**) NP-specific IgM-BCR, IgG-BCR, IgM/G chimera, or IgG/M chimera was reconstituted on the B cell lines BAL17 with retrovirus vectors. Infectants were stimulated with 0.2 μg/ml NP-BSA for the indicated times at 37°C. (**B**) Alternatively, NP-specific IgM-BCR or IgG-BCR was reconstituted on lipopolysaccharide-stimulated spleen B cells from C57BL/6 mice with retrovirus vectors and then stimulated with 10 μg/ml NP-BSA for 1 min at 37°C. Cells were lysed, and the indicated molecules were immunoprecipitated. Immunoprecipitates were subjected to Western blot analysis with anti–phospho-tyrosine (4G10). The blots were reprobed with anti-CD22, anti-CD72, or anti–SHP-1 to ensure equal loading. Alternatively, the phosphorylation level of ERK was examined by Western blotting of total cell lysates with anti–phospho-ERK. The same blot was reprobed with anti–β-tubulin to ensure equal loading. Representative data from at least three experiments are shown. Dose-response analysis on BAL17 cells is shown in fig. S5A.

uted to other factors such as their increased affinity to antigens as a result of accumulated somatic mutations of immunoglobulin during the generation of memory B cells (*24*).

References and Notes

1. M. Reth, J. Wienands, *Annu. Rev. Immunol.* **15**, 453 (1997).
2. T. Kurosaki, *Annu. Rev. Immunol.* **17**, 555 (1999).
3. S. W. Martin, C. C. Goodnow, *Nature Immunol.* **3**, 182 (2002).
4. T. F. Tedder, J. Tuscano, S. Sato, J. H. Kehrl, *Annu. Rev. Immunol.* **15**, 481 (1997).
5. L. O'Rourke, R. Tooze, D. T. Fearon, *Curr. Opin. Immunol.* **9**, 324 (1997).
6. T. Tsubata, *Curr. Opin. Immunol.* **11**, 249 (1999).
7. T. Adachi, C. Wakabayashi, T. Nakayama, H. Yakura, T. Tsubata, *J. Immunol.* **164**, 1223 (2000).
8. R. M. Tooze, G. M. Doody, D. T. Fearon, *Immunity* **7**, 59 (1997).
9. C. J. Peaker, M. S. Neuberger, *Eur. J. Immunol.* **23**, 1358 (1993).
10. C. Leprince, K. E. Draves, R. L. Geahlen, J. A. Ledbetter, E. A. Clark, *Proc. Natl. Acad. Sci. U.S.A.* **90**, 3236 (1993).
11. T. L. O'Keefe, G. T. Williams, S. L. Davies, M. S. Neuberger, *Science* **274**, 798 (1996).
12. K. L. Otipoby *et al.*, *Nature* **384**, 634 (1996).
13. S. Sato *et al.*, *Immunity* **6**, 551 (1996).
14. L. Nitschke, R. Carsetti, B. Ocker, G. Kohler, M. C. Lamers, *Curr. Biol.* **7**, 133 (1997).
15. C. Pan, N. Baumgarth, J. R. Pames, *Immunity* **11**, 495 (1999).
16. J. Wienands, J. Hombach, A. Radbruch, C. Riesterer, M. Reth, *EMBO J.* **9**, 449 (1990).
17. P. Weiser, C. Riesterer, M. Reth, *Eur. J. Immunol.* **24**, 665 (1994).
18. G. M. Doody *et al.*, *Science* **269**, 242 (1995).
19. T. Adachi, H. Flaswinkel, H. Yakura, M. Reth, T. Tsubata, *J. Immunol.* **160**, 4662 (1998).
20. Materials and methods are available as supporting material on *Science* Online.
21. M. Reth, *Annu. Rev. Immunol.* **10**, 97 (1992).
22. T. Kaisho, F. Schwenk, K. Rajewsky, *Science* **276**, 412 (1997).
23. C. Wakabayashi, Y. Takahashi, T. Takemori, T. Tsubata, unpublished data.
24. K. Rajewsky, *Nature* **381**, 751 (1996).

25. We thank M. Reth for cell lines and plasmids; L. Nitschke, T. Kitamura, G. Nolan, and H. Yakura for reagents; Y. Takahashi and T. Takemori for sharing unpublished data; and H. Fujimoto, S. Irie, and K. Mizuno for technical help. Supported by grants from the Japanese Ministry of Education, Science, Sport and Culture, and the Mochida Memorial Foundation for Medical and Pharmaceutical Research.

Supporting Online Material
www.sciencemag.org/cgi/content/full/298/5602/2392/DC1
Materials and Methods
Figs. S1 to S5
References and Notes

5 August 2002; accepted 24 October 2002

Photosynthetic Light Harvesting by Carotenoids: Detection of an Intermediate Excited State

G. Cerullo,[1]* D. Polli,[1] G. Lanzani,[1] S. De Silvestri,[1] H. Hashimoto,[2]† R. J. Cogdell[2]

We present the first direct evidence of the presence of an intermediate singlet excited state (S_x) mediating the internal conversion from S_2 to S_1 in carotenoids. The S_2 to S_x transition is extremely fast and is completed within approximately 50 femtoseconds. These results require a reassessment of the energy transfer pathways from carotenoids to chlorophylls in the primary step of photosynthesis.

Light harvesting by carotenoids is a fundamental part of the earliest reaction in photosynthesis (*1–3*). Light energy that is absorbed by carotenoids is rapidly and efficiently transferred to the chlorophylls, thereby allowing photosynthesis to harvest energy over a wider range of wavelengths than would be possible with chlorophyll alone. In some marine environments, major primary producers such as dinoflagellates survive solely on light absorbed by their carotenoids (*4*). Other than their role in photosynthesis, carotenoids are also widely studied as models for conjugated polymers (*5*) and are candidates for molecular electronics applications. Over the past decade, stimulated by the determination of several high-resolution structures of photosynthetic antenna complexes (*6*), there has been great interest in understanding the detailed mechanisms involved in the carotenoid-to-chlorophyll singlet-singlet energy transfer reaction (*3*, *7*). By using ultrafast spectroscopy to probe the very early events of energy relaxation in carotenoids, we directly demonstrate the existence of an intermediate excited state. This requires a reassessment of the current mechanistic description of the accessory light-harvesting function of carotenoids.

[1]National Laboratory for Ultrafast and Ultraintense Optical Science (INFM), Dipartimento di Fisica, Politecnico di Milano, Piazza L. da Vinci 32, 20133 Milano, Italy. [2]Division of Biochemistry and Molecular Biology, University of Glasgow, Glasgow, UK.

*To whom correspondence should be addressed. E-mail: giulio.cerullo@fisi.polimi.it
†Present address: "Light and Control," PRESTO/JST, Department of Physics, Graduate School of Science, Osaka City University, Osaka, Japan.